IMPROVED DIRECTIONAL STABILITY

IN TRACTION CONTROL SYSTEM

Hunsang Jung[1)] *, Byunghak Kwak* [2)] *, Youngjin Park* [3)]

1) Name : Hunsang Jung

Affiliation : Center for Noise and Vibration Control (NoViC), Department of Mechanical Engineering, Korea Advanced Institute of Science and Technology (KAIST), Science Town, Taejon 305-701, South Korea

Tel : 82-42-869-3076

Fax : 82-42-869-8220

E-mail : elrond@kaist.ac.kr

2) Name : Byunghak Kwak

Affiliation : Central R&D Center, Mando Corporation,

& Center for Noise and Vibration Control (NoViC), Department of Mechanical Engineering, Korea Advanced Institute of Science and Technology (KAIST), Science Town, Taejon 305-701, South Korea

Tel : 82-42-869-3076

Fax : 82-42-869-8220

E-mail : bhkwak@kaist.ac.kr

3) Name : Youngjin Park

Affiliation : Center for Noise and Vibration Control (NoViC), Department of Mechanical Engineering, Korea Advanced Institute of Science and Technology (KAIST), Science Town, Taejon 305-701, South Korea

Tel : 82-42-869-3036

Fax : 82-42-869-8220

E-mail : yjpark@sorak.kaist.ac.kr

Total number of pages: 18
Total number of tables: 0
Total number of figures: 8

Abstract

Traction control system (TCS) comprises the slip control subsystem and the directional stability subsystem. The slip controller can enhance the traction performance by maintaining the slipratio within a proper range. Additional information about the lateral behavior of the vehicle is necessary to enhance the directional stability during the cornering or lane change on the slippery roads. With an assumption of slowly varying steering input, a new method to measure the mixture of yaw rate and lateral acceleration using the speed difference of non-driven wheels is proposed. Using this measurement, the controller imposes independent pressure to each driven wheel and improves the stability during the cornering on the slippery road or acceleration on the split-μ road without additional sensors. The proposed method is verified through the simulation based on the 15 degrees of freedom passenger car model.

Introduction

Before the active control methodologies are adopted in the vehicle control, the dynamic behavior of the vehicle during the extreme situations has been controlled only by the driver's maneuver. The limit of the driver's response time and the vehicle sensitivity to the driver's mistake make the active control such as Anti-lock brake system (ABS) [1], Traction control system (TCS) [2] and Vehicle stability control (VSC) [3] necessary for safety improvement. The fast development of micro-processor helps the active control become the standard methodology for the vehicle stability. At first, ABS has been developed to prevent the wheel locking and maximize the braking force during the braking using the sensing information of the wheel velocities. TCS can cover not only the braking behavior but also the traction behavior controlling the traction torque of the engine by use of the throttle angle.

TCS comprises the slip control part and the directional stability enhancement part. The slip control part of TCS, which prevents the over-slips of the driven wheels, controls the brake pressure for the slipratio of the driven wheels to track the desired slipratio at which the maximum traction force is generated. Researchers have used the sliding mode control to regulate the slipratio under the variation of brake gain, vehicle mass and road conditions [4,5]. Jung et al. [6] designed the desired brake pressure according to the slipratio and the speed of the driven wheel and let the brake pressure tracks the desired one. Normally, these slip controllers apply the same brake pressure to the left and right driven wheels or consider the slip regulation of the one wheel.

TCS can enhance the lateral stability and the steerability of the vehicle indirectly maintaining the slipratio low to prevent the reduction of the lateral tire force. The conventional method needs the driver's excessive steering efforts because of the saturation of the lateral adhesion force during the vehicle maneuvers on the slippery road. To solve this problem, the slipratio of the driven wheels should be adjusted according to the driver's steering and the lateral movement of the vehicle to increase the lateral adhesion forces. In general, to obtain the information of the lateral vehicle movement, the measurement of the yaw rate and the lateral acceleration is necessary.

Many researchers have investigated the method of adjusting the brake pressure using the signals of these additional sensors. Park et al. [7] computed the slip angle of the driven wheels using the lateral acceleration and yaw rate sensors. They decreased the desired slipratio as the slipangle increases noticing the fact that the lateral force decreases as the slipangle increases. Alberti et al. [8] distributed individual brake pressures to the tires to balance the yaw-directional moment using the estimated slipangle.

All of these methods require expensive additional sensors. These additional sensors are essential to estimate the transient responses by the sudden and rapid steering input such as the obstacle avoidance. But if the control target for the lateral dynamics is restricted to the cases of slow steering input or constant steering angle, the transient response of the lateral dynamics can be neglected and the steady state characteristics of the vehicle by the steering input can be used to estimate the behavior of the vehicle. The normal situations that the drivers confront during cornering or acceleration on the split-μ road belong to these cases.

Our objective is to develop a novel approach that can enhance the lateral stability during the course tracking on the slippery road or the split-μ road without use of additional sensors. Using the steady state characteristics of the lateral dynamics, a new method to estimate the mixture of yaw rate and lateral acceleration using the speed difference of the left and right non-driven wheels without using the lateral acceleration and yaw rate sensors is proposed. A control scheme that applies independent brake pressure to each driven wheel according to this measure is designed as well. Brake pressures of the driven wheels are adjusted according to the driver's steering input to improve the directional stability increase in the case of cornering and acceleration on the split-μ road. The proposed method is validated using the 15 DOF nonlinear vehicle model.

Vehicle Modeling

The vehicle model shown in Figure.1 consists of chassis, tire and brake. Each part is important to monitor the performance of TCS and is simplified as much as possible. Chassis model is of 15 DOF, where 6 DOF are for sprung mass, 4 DOF are for suspensions ,4 DOF are for wheel rotation and 1 DOF is for steering. UA tire model is employed since it shows similar characteristics to the real tire for various slipratios, slip angles and road conditions. This nonlinear model is verified by real vehicle test for the impulse and the step steering [9].

The brake system consists of master cylinders and TCS modulators which make up the pressure source and the brake cylinder that applies the brake pressure to the wheels. The solenoid valves of brake cylinders repeat on/off motion forming the brake pressure. Dynamics of the brake cylinder pressure can be represented as follows [10]:

$$\frac{V_b}{\beta}\dot{P}_b = c_1 x_1 \sqrt{\frac{2}{\rho}\left(P_m - P_b\right)} - c_2 x_2 \sqrt{\frac{2}{\rho}P_b}, \tag{1}$$

where $V_b, \beta, c_i, P_m, \rho$ and x_i are the brake cylinder volume, the fluid volume coefficient, the valve constant, the master cylinder pressure, the fluid density and the solenoid distance, respectively. The master cylinder pressure, P_m is always assumed to be ready and the dynamics of TCS modulator is omitted.

The estimation of Ψ

The slipangle of the non-driven wheel changes according to the steering input and the vehicle state, but the slipratios of the non-driven wheels stay around zero. If the rolling radius of the non-driven wheel is known and the rotational speed can be measured, it is possible to compute the velocity of tire center on the traveling direction of wheels. The left and right center velocities of non-driven wheels are as follows:

$$\tilde{\omega} = \omega_x \tilde{x} + \omega_y \tilde{y} + \omega_z \tilde{z} \tag{2}$$

$$OR = L_1 \tilde{x} + L_2 \tilde{y} - L_{3R} \tilde{z} \quad , \quad OL = L_1 \tilde{x} - L_2 \tilde{y} - L_{3L} \tilde{z} \tag{3}$$

$$\tilde{V}_L = \tilde{V}_O + \tilde{\omega} \times L = \left(V_x - L_{3L}\omega_y - \omega_z L_2\right)\tilde{x} + \left(V_y + L_{3L}\omega_x + L_1\omega_z\right)\tilde{y} + \left(L_2\omega_x - L_1\omega_y\right)\tilde{z} \tag{4}$$

$$\tilde{V}_R = \left(V_x - L_{3R}\omega_y + \omega_z L_2\right)\tilde{x} + \left(V_y + L_{3R}\omega_x + L_1\omega_z\right)\tilde{y} - \left(L_2\omega_x + L_1\omega_y\right)\tilde{z} \ , \tag{5}$$

where $\tilde{\omega}$, OR and OL are the angular velocities of the vehicle, the distances from the mass center of the vehicle to the center of right and left non-driven wheels, respectively. The velocity of the mass center, $\tilde{V}_o$ comprises V_x, V_y and V_z. $\tilde{V}_R$ and $\tilde{V}_L$ are the center velocity of the right and left non-driven wheels, respectively in the SAE xyz coordinates as shown in Figure 2. The velocities of tire centers in the traveling direction of wheels in the transformed coordinates $\left(x'y'\right)$ by the steering angle, α are as follows:

$$V_{Lx'} = \left(V_x - L_{3L}\omega_y + \omega_z L_2\right)\cos\alpha + \left(V_y + L_{3L}\omega_x + L_1\omega_z\right)\sin\alpha \tag{6}$$

$$V_{Rx'} = \left(V_x - L_{3R}\omega_y - \omega_z L_2\right)\cos\alpha + \left(V_y + L_{3R}\omega_x + L_1\omega_z\right)\sin\alpha\,. \tag{7}$$

It is noted that the difference of two values is mostly due to the yaw rate $\left(\omega_z\right)$. The difference of the $V_{Lx'}$ and $V_{Rx'}$ is as follows:

$$V_{Lx'} - V_{Rx'} = 2L_2\omega_z\cos\alpha + \left(L_{3R} - L_{3L}\right)\omega_y\cos\alpha + \left(L_{3R} - L_{3L}\right)\omega_x\sin\alpha\ . \tag{8}$$

Assuming $L_{3R} \approx L_{3L}$, the following approximation can be derived.

$$V_{Lx'} - V_{Rx'} = r_L\omega_L - r_R\omega_R \cong 2L_2\omega_z\cos\alpha\ . \tag{9}$$

If we can measure the rolling radii of non-driven wheels, the yaw-rate can be estimated using the equation (9). The fundamental cause of the radius difference of the left and right wheels is the load change due to the transmission of the lateral acceleration through the suspension. The transient response of load change is due to the suspension dynamics. If the cases of small variation of the steering input are considered, the transient response of the suspension can be assumed to be negligibly fast. So the steady state change of rolling radii by the lateral acceleration ignoring the suspension dynamics is as follows:

$$N = \frac{m\cdot H}{2L_{wt}}a_y \tag{10}$$

$$r_R = r_s + \frac{N}{K_t}\ ,\ \ r_L = r_s - \frac{N}{K_t}\ , \tag{11}$$

where N, r_s, L_{wt}, H and K_t are the dynamic load on each suspension, the initial radius of the non-driven wheels, the wheel tread and the distance from the roll center to the vehicle center and the tire stiffness as shown in Figure 3. We assume r_s is known and the change of the rolling radii can not be measured. The left side of the equation (9) can be divided into the term of ω_L, ω_R and r_s of which values are known and the other term as shown in equation (12).

$$V_{Lx'} - V_{Rx'} = r_L\omega_L - r_R\omega_R = r_s\left(\omega_L - \omega_R\right) - K_v\left(\omega_L + \omega_R\right)a_y \cong 2L_2\omega_z\cos\alpha\ , \tag{12}$$

where $K_v = m\cdot H/2L_{wt}K_t$. Modifying the equation (12), we can define Ψ, the estimate of yaw rate as follows:

$$\Psi = \frac{r_s(\omega_L - \omega_R)}{L_{wt}\cos\alpha} \cong \omega_z + \frac{K_v(\omega_L + \omega_R)}{L_{wt}\cos\alpha} \cdot a_y \quad . \tag{13}$$

The measure defined as Ψ includes the effect of the steady-state yaw rate and the lateral acceleration. If one of the yaw rate sensor and lateral acceleration sensor is available for use, the other can be estimated using the equation (13) in the steady state. In this research, it is assumed that both of the sensors are not equipped in the normal TCS vehicle. In Figure 4, the yaw rate is compared with Ψ where the 45 deg step steering input is applied to the vehicle with constant speeds. In normal cases, the yaw rate is almost equal to the estimated value up to 10km/h since the lateral acceleration is low at low velocity. But, the error increases as the speed goes up. When the vehicle speed is 30 km/h and 50 km/h, 25% and 100% error are occurred, respectively. Hence, we know that Ψ can be used as the estimate of the yaw rate at very low speed. But, at high speed, Ψ is different from the yaw rate by the effect of the lateral acceleration and is the weighted summation of the yaw rate and the lateral acceleration. It will be shown through the simulation, if Ψ is regulated to the desired value, both of the yaw rate and the lateral acceleration are regulated. Ψ_d , the desired value of Ψ is necessary to design a directional stability controller based on the Ψ feedback. For this reason, it is necessary to calculate not only the desired yaw rate but also the desired lateral acceleration.

The computation of Ψ_d

To compute the desired yaw rate and lateral acceleration, it is assumed that drivers expect the normal behavior with which they are familiar even in the extreme driving conditions. In this case, the desired yaw rate and lateral acceleration can be computed from the linear vehicle model that has the yaw rate and the lateral acceleration as states.

$$\begin{cases} I_z \dot{\omega}_z = l_f F_{yf} - l_r F_{yr} \\ m\left(\dot{V}_y + V_x \cdot \omega_z\right) = F_{yf} + F_{yr} \end{cases} . \tag{14}$$

Lateral force $F_{y(.)}$ is decided from the equivalent cornering stiffness and the slip angle as follows:

$$F_{yf} = 2K_f \cdot \alpha_f \quad , \quad F_{yr} = 2K_r \cdot \alpha_r \quad , \tag{15}$$

where $\alpha_{(.)}$ is derived from the difference of steering angle and slip angle. Subscripts f and r represent the front and rear tire, respectively.

$$\begin{aligned} &\alpha_f = \delta_f - \beta_f \quad , \ \alpha_r = -\beta_r \\ &\beta_f = \beta + l_f \cdot \frac{\omega_z}{V_x} \ , \ \beta_r = \beta - l_r \cdot \frac{\omega_z}{V_x} \end{aligned} \quad . \tag{16}$$

Using the steady state assumption,

$$\omega_{zd} = \frac{V_x \delta_f}{L_{wb}\left(1 + KV_x^2\right)}, \quad a_{yd} = V_x \cdot \omega_{zd} = \frac{V_x^2 \delta_f}{L_{wb}\left(1 + KV_x^2\right)} \quad , \tag{17}$$

where $K = m\left(l_r K_r - l_f K_f\right) / 2L_{wb}^2 K_f K_r$. K may be derived from the simulation result using the nonlinear vehicle model as well. Now we can define the Ψ_d using the desired yaw rate and lateral acceleration as follows :

$$\Psi_d = \omega_{zd} + \frac{K_v\left(\omega_L + \omega_R\right)}{L_{wt}\cos\alpha} \cdot a_{yd} \quad . \tag{18}$$

Controller Structure

The controller schematics proposed in this manuscript is shown in Figure 5. Note that the additional brake pressure, P_a is made using $\Psi - \Psi_d$. P_a is added to the desired brake pressure computed from the fundamental slip controller [6] to the appropriate wheel following the rules in equations (19) and (20). The brake pressures of the left and right driven wheels become different. Normally the brake pressure distribution based on the yaw rate sensing alone makes the vehicle track the desired yaw rate well but when the lateral force is not sufficient the vehicle may drift away from the course as the slip angle becomes large [9]. In the proposed method, both of the lateral acceleration and the yaw rate goes to the desired values and this problem can be alleviated.

$$\begin{aligned} P_a &= K_b \cdot \left(\Psi - \Psi_d\right) \\ &= K_b \cdot \left(\left(\omega_z - \omega_{zd}\right) + \frac{K_v\left(\omega_L + \omega_R\right)}{L_{wt} c\alpha} \cdot \left(a_y - a_{yd}\right)\right) \end{aligned} \tag{19}$$

$$\begin{aligned} &\text{if } \Psi - \Psi_d > 0 \Rightarrow P_{des/L} = P_{des} + P_a \ , P_{des/R} = P_{des} \\ &\text{if } \Psi - \Psi_d \le 0 \Rightarrow P_{des/R} = P_{des} + P_a \ , P_{des/L} = P_{des} \end{aligned} , \tag{20}$$

where $P_{des/L}$ and $P_{des/R}$ are the desired brake pressure of left and right driven wheels, respectively.

The simulation result

In the equation (12), parameter K_v includes vehicle mass, m, the distance from the roll center to the vehicle mass center, H, and the tire stiffness, K_t. When the vehicle mass increases, the tire stiffness also increases because of the nonlinear characteristics of the tire and H also varies according to the driving conditions. K_v deviates from the nominal value and the nonlinear characteristics appear in the case of cornering or lane change. To validate the proposed controller in this circumstance, the cornering characteristics of the vehicle on the slippery roads and the start off characteristics of the vehicle on the split-μ road are investigated. Detailed implementation of the brake pressure and the throttle angle is explained in [6].

Cornering characteristics

The vehicle is assumed to accelerate on the curve with 40m radius at the initial speed of 30km/h. The desired slipratio of the fundamental slip controller is designed as –0.2 in this case. The driver model is omitted. It is assumed that the driver does not consider the vehicle status, and applies the steering to the vehicle according to the current speed in order to track the course with constant radius. The steering input is obtained from the steady state reference yaw rate equation shown as follows.

$$\omega_{zd} = \frac{V_x \delta_f}{L_{wb}\left(1+KV_x^2\right)} = \frac{V_x}{R} \tag{21}$$

$$\delta_f = \frac{L_{wb}\left(1+KV_x^2\right)}{R}. \tag{22}$$

Then the driver’s steering varies from the initial 46 degree to the final 51 degree after 10 sec.

As additional brake pressure by the directional stability controller is applied to the right driven wheel, the longitudinal acceleration of the vehilce is decreased as the slip ratio of the right wheel is decreased below –0.2 as shown in Figure 6(a) and (b). That is, the yaw-directional moment of the vehicle is preserved as the traction force of right driven wheel decreases because of the additional brake torque generated by the Ψ feedback. Though the acceleration decreases, the yaw rate and the lateral acceleration track the desired values within permitable error bounds as shown in Figure 6(c) and (d). The vehicle with the proposed controller tracks the desired path and the driver’s additional steering is not necessary. But the conventional TCS vehicle with the conventional controller which applies the same brake pressure to the left and right driven wheels with fixed target slipratio could not track it and spun out.

Start off on the split-μ road

Another important measure for the directional stability is the acceleration performance on the split-μ roads without driver’s additional steering. Simulation is performed on the condition that the throttle angle maximally increases on the road where μ of the right road is 0.3, snowy road, and μ of the left road is 0.1, icy road. Without the controller, the lateral adhesion forces decrease as the slips are generated in the left and right driven wheels as in Figure 7(b). If the driver does not attempt the corrective steering in this condition, the vehicle spins out to the direction of low μ road and, then, leaves the desired course. But the vehicle with the proposed controller tracks the course as the controller imposes the additional brake pressure to the right wheel without the driver's intervention as shown in Figure 7(c).

The variation of K_v

All of the above simulation results are conducted on the condition that the variable K_v in the equation (12) is known exactly. From the equation (12), K_v can vary when the vehicle mass increases. So it is necessary to observe the cornering performance if K_v used in the controller is different from the actual value. The next simulation result is the case when nominal K_v used in the controller varies $\pm 20\%$ from the actual one. Tracking performance of the yaw rate and lateral acceleration shown in Figures 8(a) and (b) demonstrates that the total cornering performance does not vary much from the nominal case.

Conclusion

The objective of this research is to design the TCS controller to enhance the direction stability. To insure the directional stability without using additional sensors, a new method to compute the mixture of yaw rate and lateral acceleration using the steady state information of lateral dynamics is proposed. Additional brake pressure proportional to this measure is applied to the left and right driven wheels conditionally. The proposed controller is verified with simulations based on 15 DOF passenger car model. The resolution and frequency limit of the sensors used for speed detection of the wheels and the nonlinear dynamics of the chassis which is not considered in the simulation model can influence the controller performance. Therefore, further study based on the experiment is needed to check the feasibility of the proposed controller.

Reference

1 **Masaru Sugai, Hiroyuki Yamaguchi, Masanori Miyashita, Takaji Umeno and Katsuhiro Asano**, New Control Technique for Maximizing Braking Force on Antilock Braking System, *Vehicle System Dynamics*, 1999,

32, 299~312

2 **Asami, K., Nomura, Y. and Naganawa, T.**, Traction Control (TRC) System for 1987 Toyota Crown. *SAE paper 890933*

3 **Anton van Zanten, Rainer Erhardt and Georg Pfaff, VDC,** The vehicle dynamics control system of Bosch, *SAE paper 950759*

4 **Tan, H.S. and Chin, Y. K.**, Vehicle antilock braking and traction control :a theoretical study, *Int. J. of Systems science*, 1992, 23(3), 351~365

5 **Choi, S. H. and Cho, D. W.**, Control of Wheel Slip Ratio Using Sliding Mode Controller with Pulse Width Modulation, *Vehicle System Dynamics*, 1999, 32, 267~284

6 **Hun Sang Jung, Byunghak Kwak, Youngjin Park**, Development of Traction Control System, *Seoul 2000 FISITA World Automotive Congress*, 2000, F2000G345

7 **Park, J. H. and Kim, C.Y.**, Wheel slip control in traction control system for vehicle stability, *Vehicle system dynamics*, 1999, 31, 263~278

8 **V. alberti and E. Babbel**, Improved driving stability by active braking of the individual wheels, *AVEC '96*, 1996, 717~731

9 **Byunghak Kwak, Youngjin Park, Dongshin Kim**, Design of Observer for Vehicle Stability Control System, *Seoul 2000 FISITA World Automotive Congress*, 2000, F2000G328

10 **H. E. Merritt,** Hydraulic Control Systems. New York: Willey, 1967

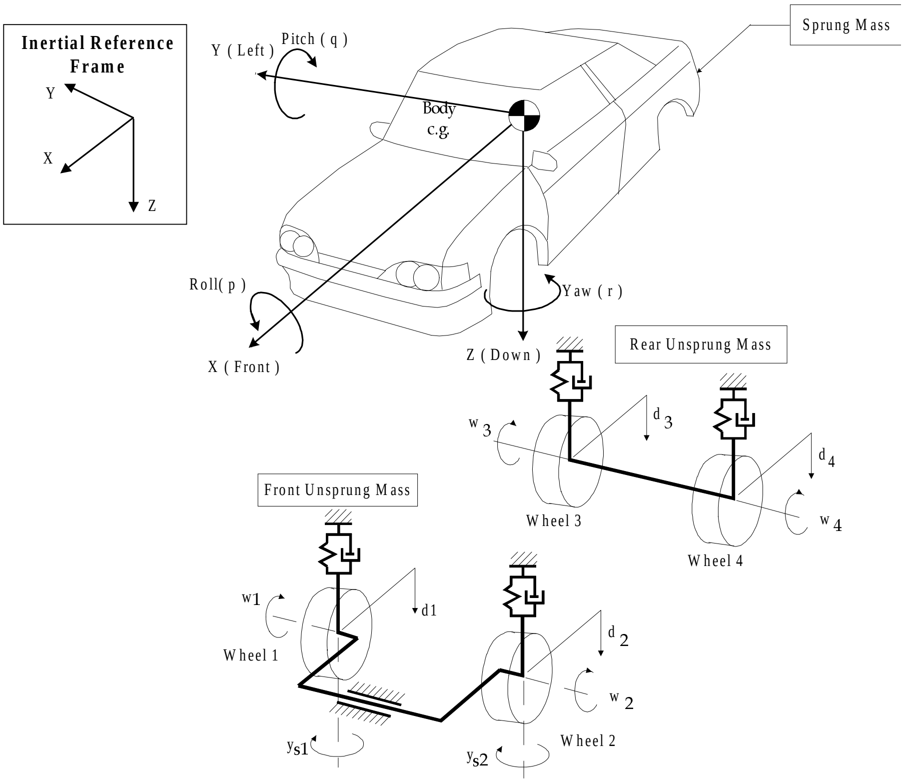

Figure 1. 15 DOF vehicle model

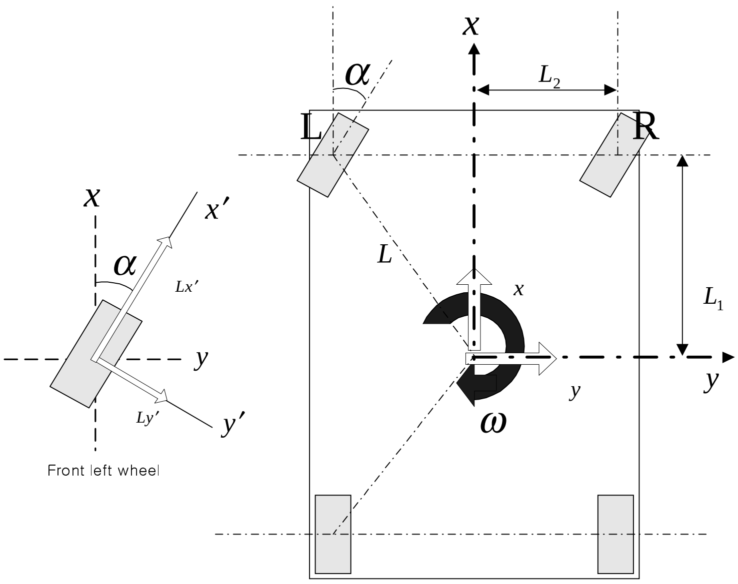

Figure 2. The center velocities of front wheels

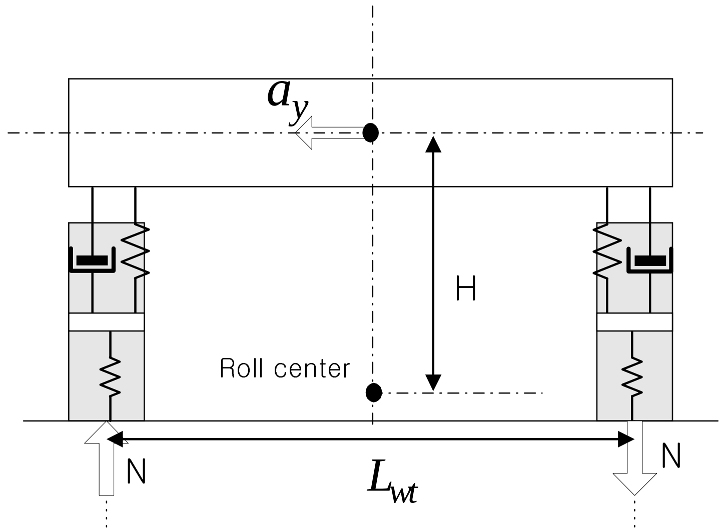

Figure 3. Normal load change by lateral acceleration

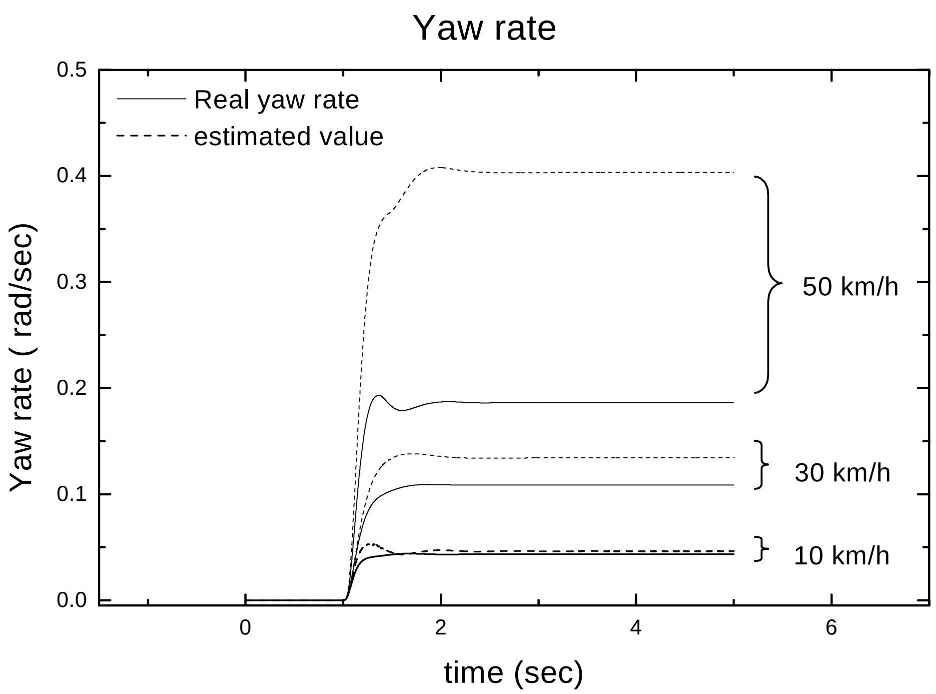

Figure 4. Yaw rate and the estimated value

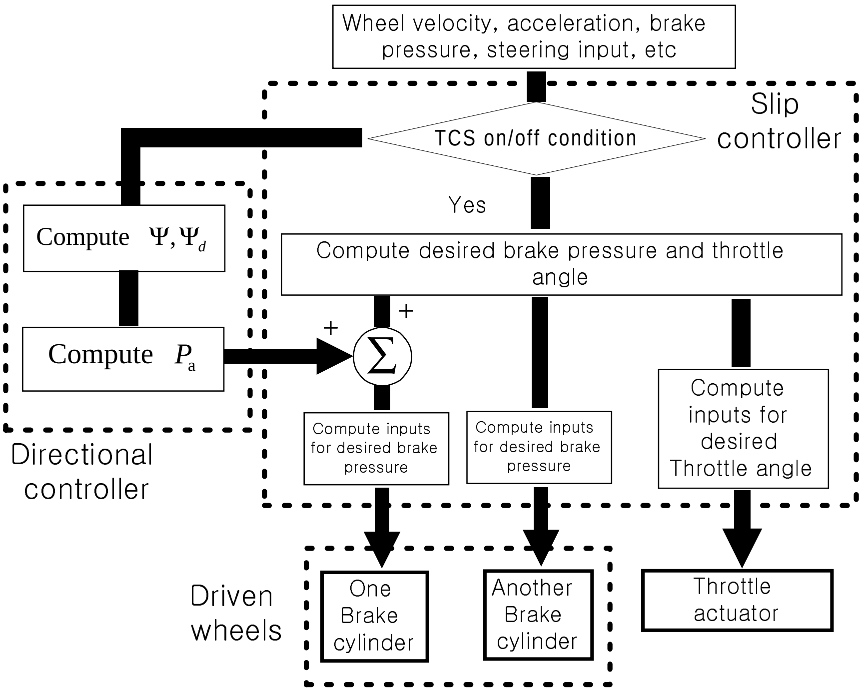

Figure 5. The controller structure

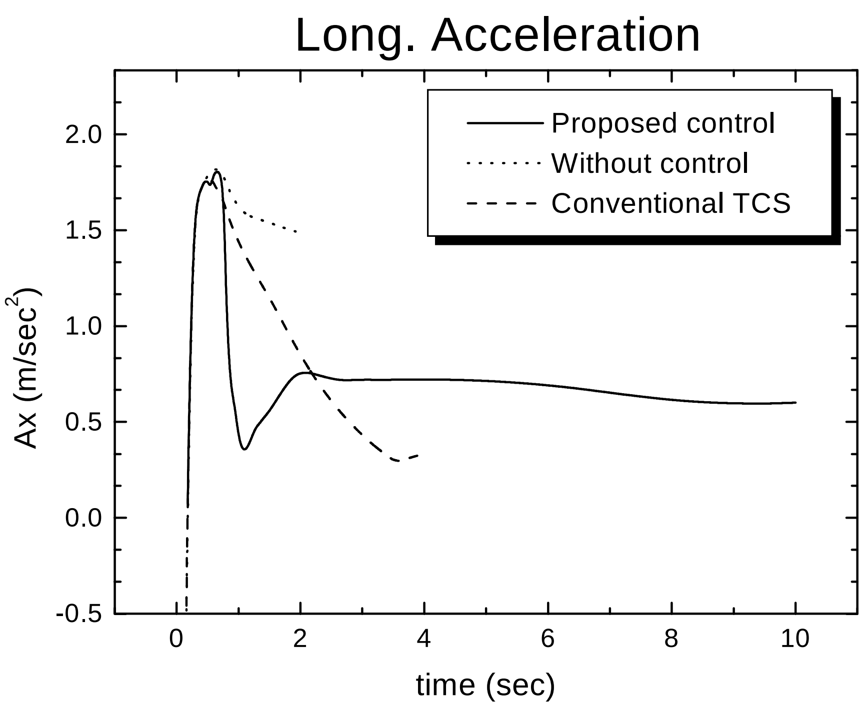

(a) Longitudinal acceleration

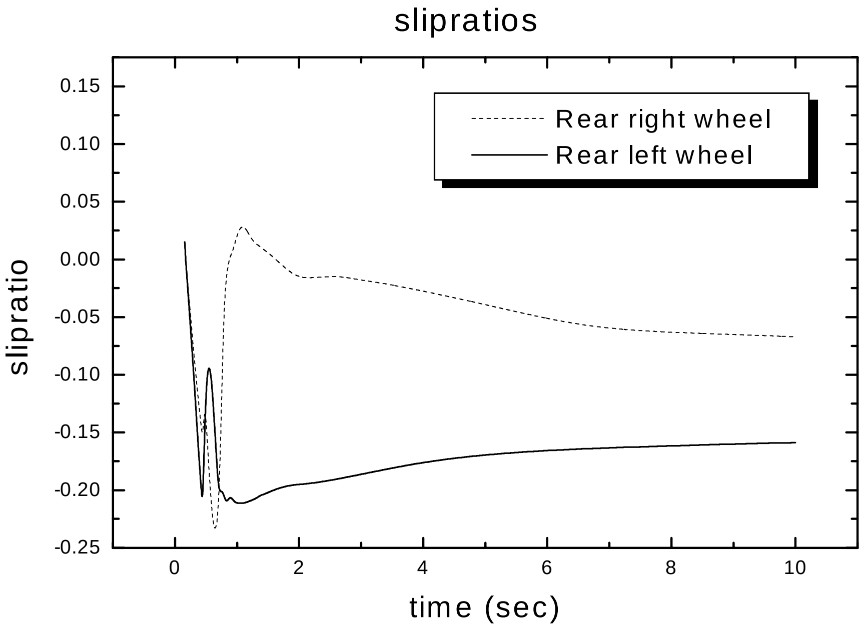

(b) Slip ratio

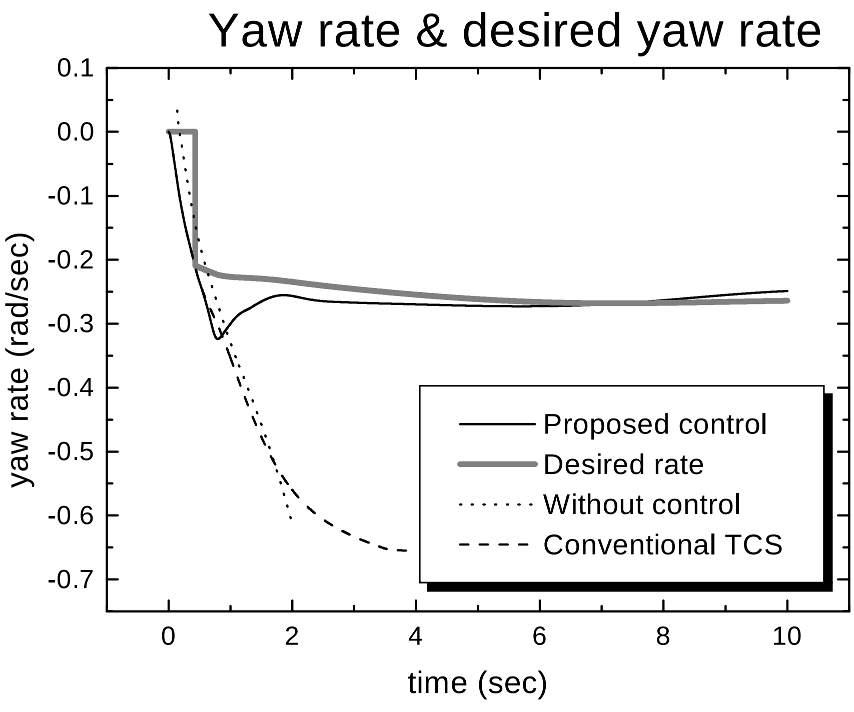

(c) Yaw rate & desired yaw rate

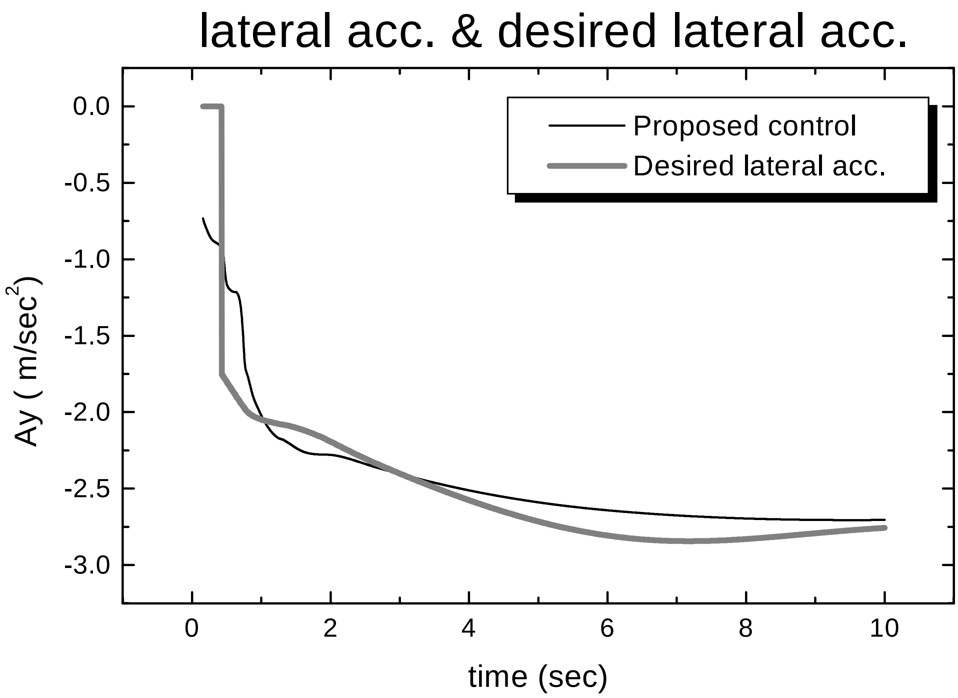

(d) Lateral acceleration & desired lateral acceleration

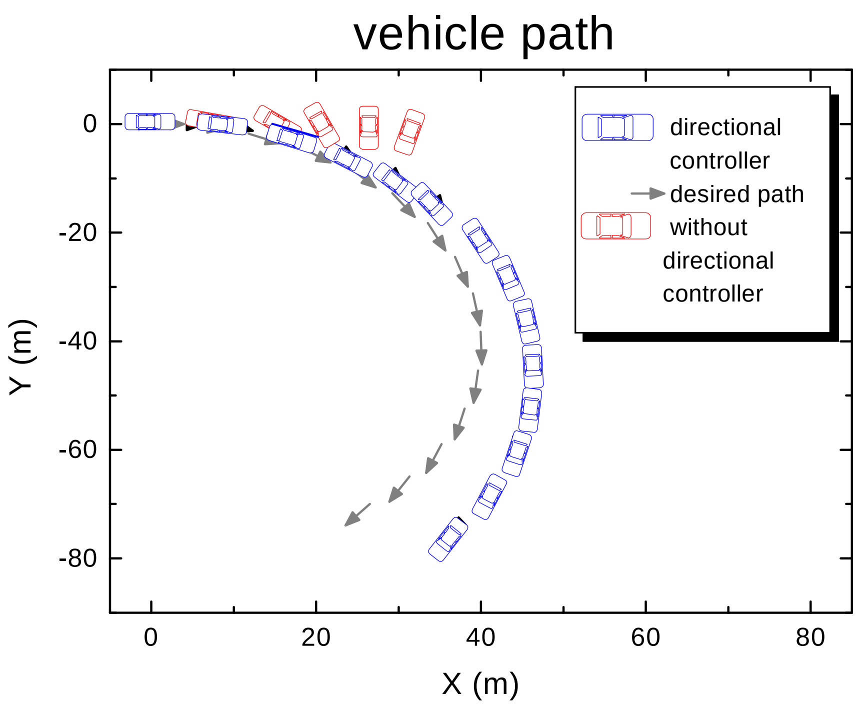

(e) Vehicle path

Figure 6. The Cornering characteristics

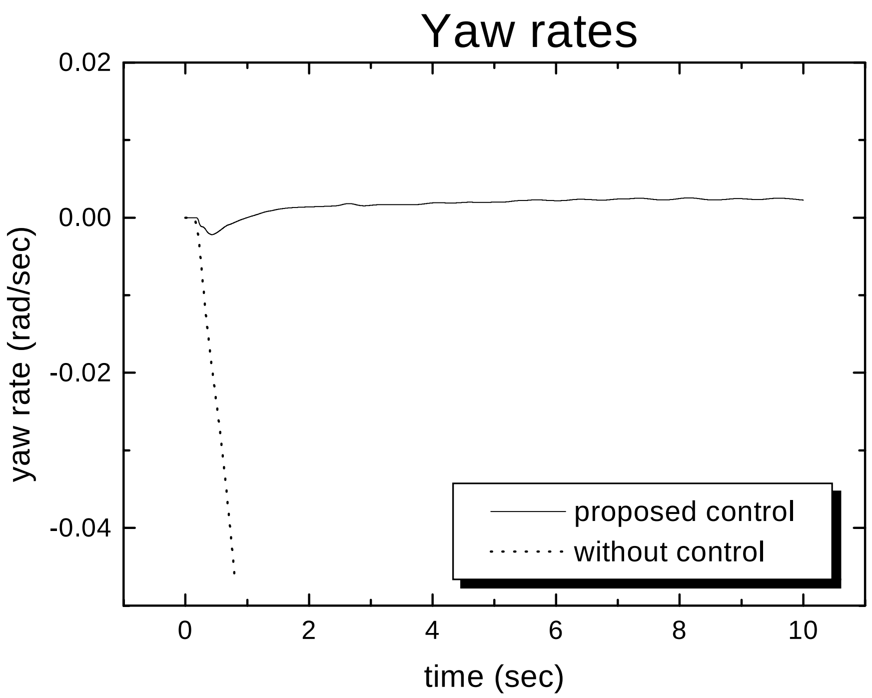

(a) Yaw rates

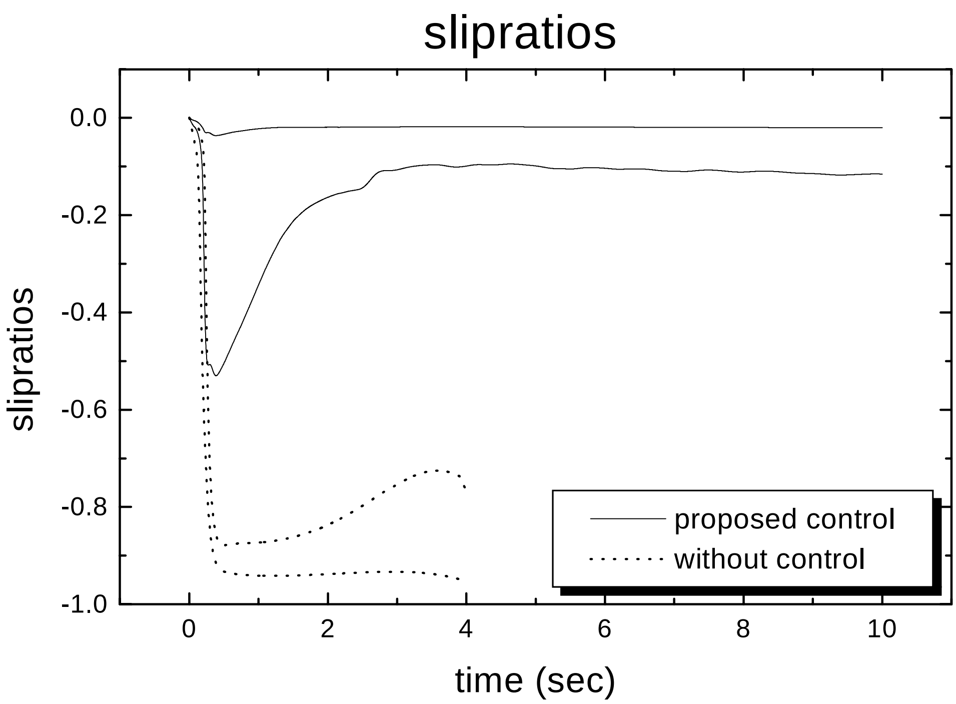

(b) Slipratios of driven wheels

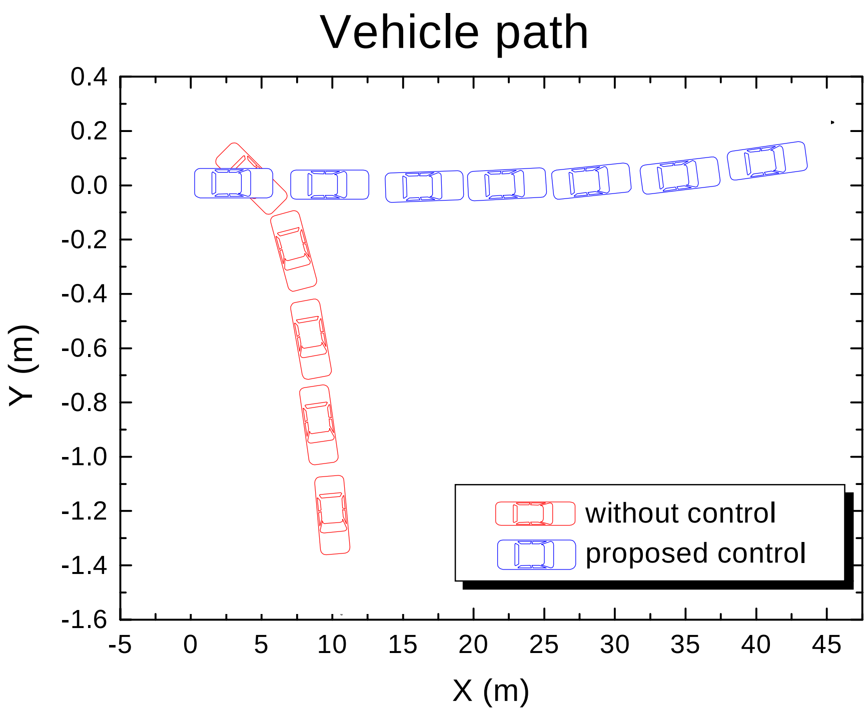

(c) Vehicle path

Figure 7. The start off on the split-μ road

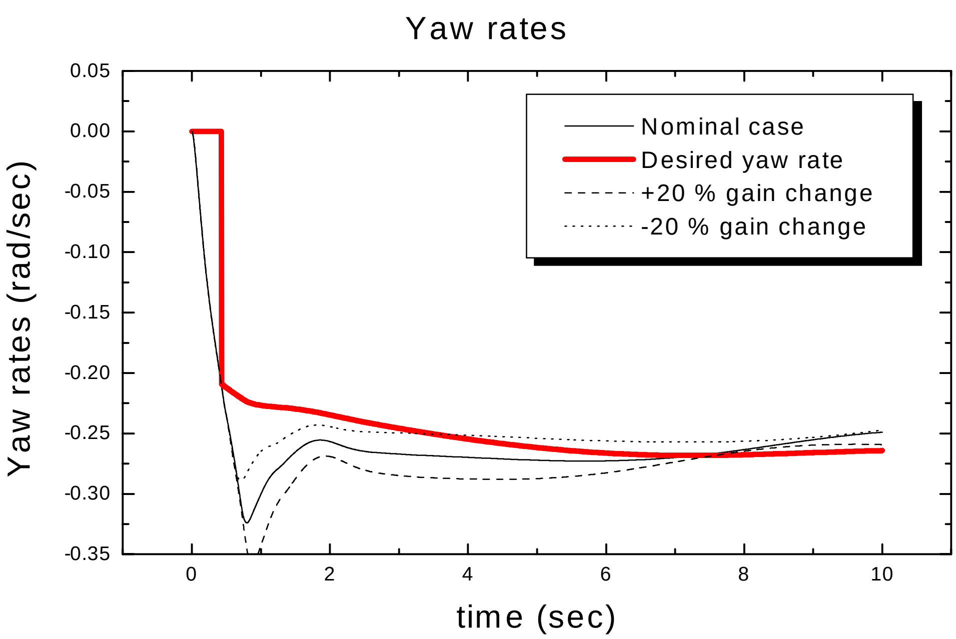

(a) Yaw rates

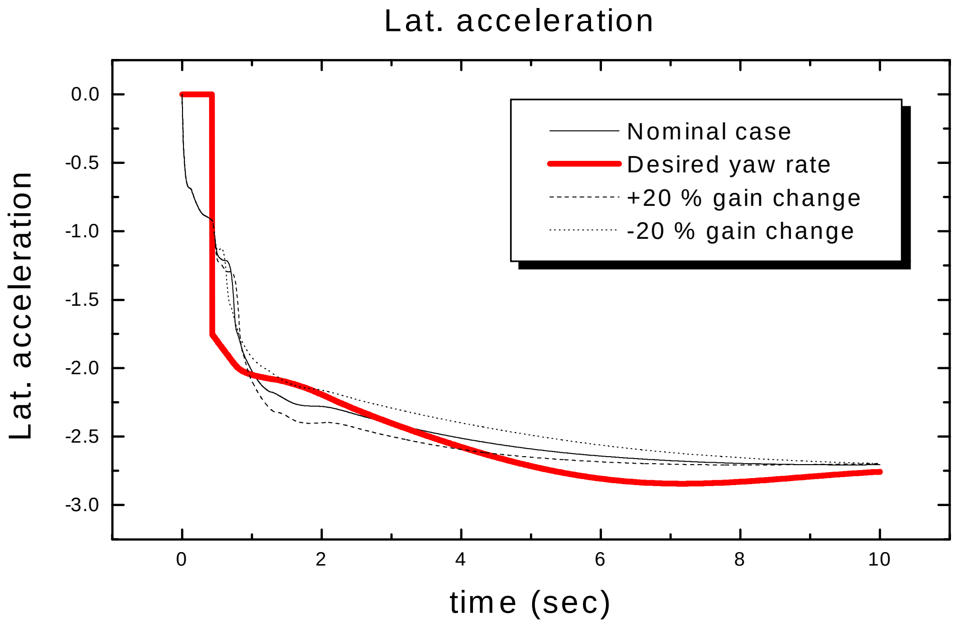

(b) Lateral accelerations

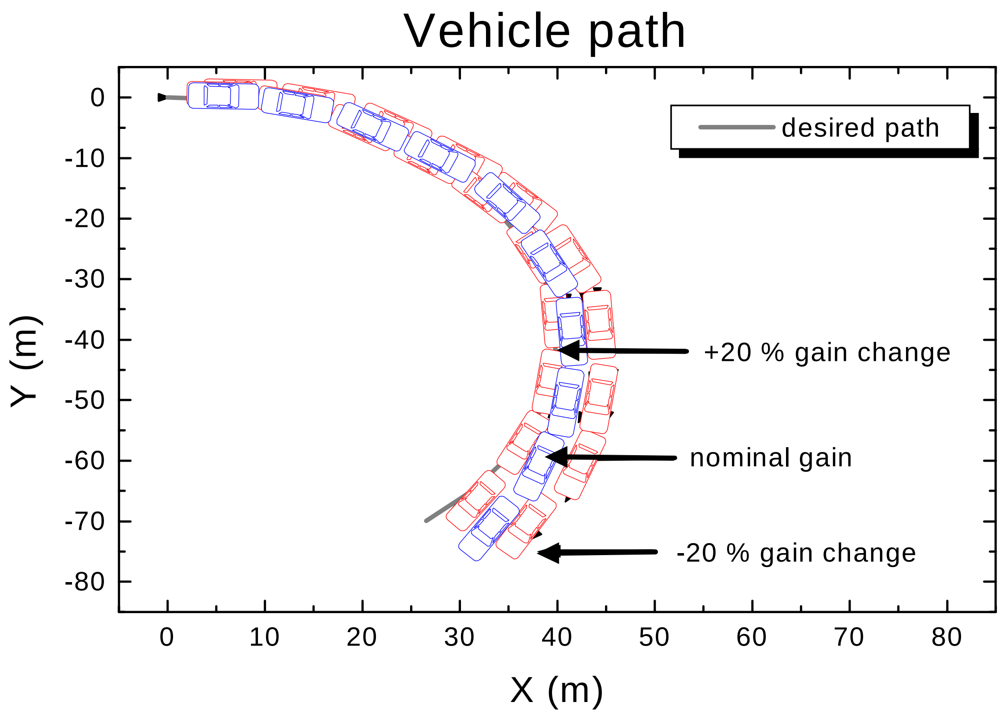

(c) Vehicle path

Figure 8. The variation of K_v